Redox dynamics in the active layer of an Arctic headwater catchment; examining the potential for transfer of dissolved methane from soils to stream water

Redox dynamics in the active layer of an Arctic headwater catchment; examining the potential for transfer of dissolved methane from soils to stream water.

Lorna E Street[1,2], Joshua F. Dean[3,4], Michael F. Billett[3], Robert Baxter[5], Kerry J. Dinsmore[6], Jason S. Lessels[7], Jens-Arne Subke[3], Doerthe Tetzlaff[7], and Philip A. Wookey[1]

[1]School of Life Sciences, Heriot-Watt University, Edinburgh EH14 4AS, UK

[2]School of GeoSciences, University of Edinburgh, Edinburgh, EH9 3FF, UK (corresponding)

[3]Biological and Environment Sciences, School of Natural Sciences, University of Stirling, Stirling FK9 4LA, UK

[4]Earth and Climate Cluster, Faculty of Earth and Life Sciences, Vrije Universiteit Amsterdam, 1081 HV Amsterdam, the Netherlands

[5]School of Biological and Biomedical Sciences, University of Durham, Durham DH1 3LE, UK

[6]Centre for Ecology and Hydrology, Bush Estate, Penicuik EH26 0QB, UK

[7]Northern Rivers Institute, School of Geosciences, University of Aberdeen, Aberdeen AB24 3UF, UK

Key points:

1. Methane formed in saturated soils above permafrost can influence surface water methane budgets via soil water discharge
2. We show novel data on redox dynamics and methane in hillslope permafrost soils and the potential for transport to streams

3. Hillslope soils become anoxic as thaw deepens and methane content increases but we find no evidence of a link to stream methane

Abstract. The linkages between methane production, transport and release from terrestrial and aquatic systems are not well understood, complicating the task of predicting methane emissions. We present novel data examining the potential for the saturated zone of active layer soils to act as a source of dissolved methane to the aquatic system, via soil water discharge, within a headwater catchment of the continuous permafrost zone in Northern Canada. We monitored redox conditions and soil methane concentrations across a transect of soil profiles from mid-stream to hillslope, and compare temporal patterns in methane concentrations in soils to those in the stream. We show that redox conditions in active layer soils become more negative as the thaw season progresses, providing conditions suitable for net methanogenesis, and that redox conditions are sensitive to increased precipitation during a storm event - but only in shallower surface soil layers. Whilst we demonstrate that methane concentrations at depth in the hillslope soils increase over the course of the growing season as reducing conditions develop, we find no evidence that this has an influence on stream water methane concentrations. Sediments directly beneath the stream bed, however, remain strongly reducing at depth throughout the thaw season, and contain methane at concentrations five orders of magnitude greater than those in hillslope soils. The extent of sub-streambed methane sources, and the rates of methane transport from these zones, may therefore be important factors determining headwater stream methane concentrations under changing Arctic hydrologic regimes.

Key words: Methanogenesis, permafrost, hydrological processes, riparian, hyporheic zone, Trail Valley Creek

1 Introduction

Surface waters in high latitude permafrost regions act as hot spots of methane emissions [*Walter et al.*, 2006; *Flessa et al.*, 2008; *Bastviken et al.*, 2011] . Lakes and ponds are estimated to account for two-thirds of natural land-surface methane sources in the boreal region northward [*Wik et al.*, 2016]. Methane release from surface waters can occur via multiple pathways; as bubbles from deeper waters or sediments (ebullition) [*Baulch et al.*, 2011; *Crawford et al.*, 2014b], via transport through the tissues of aerenchymatous plants [*Le Mer and Roger*, 2001; *King and Reeburgh*, 2002], or as a result of diffusive release (degassing) of methane dissolved in the water column [*Kling et al.*, 1992; *Billett and Moore*, 2008; *Dinsmore et al.*, 2009]. Lakes and pond waters are often super-saturated with methane with respect to the atmosphere and diffusive fluxes are a significant methane release pathway [*Kling et al.*, 1992; *Knoblauch et al.*, 2015], although in lakes ebullition fluxes are usually larger [*Sepulveda-Jauregui et al.*, 2015]. Stream systems have been much less well-studied, but can also act as conduits of methane to the atmosphere, thereby playing a potentially important role in catchment greenhouse gas budgets. For example, in boreal Alaska, methane efflux (primarily via diffusion) from a headwater stream network was estimated to account for up to 10 % of terrestrial methane sources, despite accounting for < 0.2 % of the catchment surface area [*Crawford et al.*, 2013]. Furthermore, the presence of high concentrations of dissolved methane in both lakes and streams has ecological significance as methane can support freshwater productivity via methanotrophic pathways [*Medvedeff and Hershey*, 2013; *Hershey et al.*, 2015]. We understand very little, however, about the origins of dissolved methane in freshwaters; the mechanisms driving dissolved methane dynamics and the importance of linkages between terrestrial and aquatic systems; this is especially true for headwater catchments, where the role of terrestrial-freshwater coupling assumes particular significance [*Wrona et al.*, 2016].

Transport of dissolved methane from soils into lakes and streams via shallow groundwater discharge has been implicated as an important source of methane to the aquatic system [*Kling et al.*, 1992; *Jones and Mulholland*, 1998; *Crawford et al.*, 2014a]. In their Alaskan study, Crawford *et al.* [2013] identified regions of the stream which were consistently elevated in methane concentrations, implying an important role for discreet inflows of methane-rich groundwater. It is reasonable to expect that the transfer of methane from terrestrial sources to the aquatic system may be particularly important in permafrost regions, where the presence of permafrost gives rise to a carbon-rich water-saturated zone which can provide conditions favourable to methane production [*Treat et al.*, 2015]. For example, in an Alaskan lake, discharge of methane enriched soil water from surrounding active layer soils has been shown to significantly influence methane concentrations in the lake water [*Paytan* et al., 2015]. The potential importance of dissolved methane sources and transport pathways for headwater stream systems in permafrost regions is still largely unknown, but this knowledge is important for our understanding of the functioning of freshwater systems and their role as methane emission hotpots under a future Arctic climate. Understanding the role of terrestrial sources in aquatic methane budgets is challenging however, because it requires both an understanding of potential source areas within the landscape, as well as the transport processes operating at the terrestrial-freshwater interface.

Biological processing of organic matter is dominated by redox reactions, and soil redox potential (Eh) is a critical environmental control over methanogenesis [*Husson*, 2012]. The presence of a saturated soil zone above permafrost can potentially result in the strongly reducing conditions necessary for methane production [*Peters and Conrad*, 1996], however, the relationship between soil moisture content and redox potential is complex [*McNicol and Silver*, 2014]. It takes time for oxygen to be depleted and input of oxygenated water via precipitation or lateral flow can prevent reducing conditions from developing [*Hall* et al.,

2012]. In wetland systems water table position is the primary factor controlling soil redox states [*Kettunen* et al., 1999; *Seybold* et al., 2002], however, if lateral flows dominate catchment hydrology then soil redox potential and water table depth become decoupled [*Mitchell and Branfireun*, 2005]. In permafrost regions there is very little understanding of redox dynamics associated with the seasonal development of the thaw front, in spite of its obvious significance for biogeochemical processing and patterns of methane production [*Lipson* et al., 2015]. Time-series (or indeed any) data on the redox status of Arctic soils and sediments are rarely available. Changes in dominant hydrological processes associated with climate change and deepening of the active layer [*Tetzlaff* et al., 2015] may alter redox conditions in permafrost soils and subsequent delivery of methane to the aquatic system, so it is important to understand hillslope redox dynamics and how they relate to redox-sensitive biogeochemical processes.

The lack of available data to quantify temporal and spatial patterns in soil redox potentials in permafrost systems is likely the result of a combination of the logistical challenges of working in remote regions, and a view among researchers that soil redox potential measurements are only semi-quantitative. This criticism arises from important difficulties involved in interpreting redox potential data. These limitations have been reviewed in detail elsewhere [*Grundl*, 1994; *Fiedler et al.*, 2007] but we highlight here two key points which complicate data interpretation: 1) in ideal chemical systems (i.e. in pure solutions at low ionic strength), the redox potential for any particular redox couple is determined by the activities (concentrations) of each reactant via the Nernst equation [*Skoog et al.*, 1996]. Soils, however, are a complex, spatially heterogeneous, mixture of multiple redox couples in both solid and liquid phase, at unknown activities and at chemical disequilibrium [*Grundl*, 1994]. As a result, redox potentials cannot be interpreted in a quantitative way based on thermodynamic principles, and this includes standardising measured Eh values for soil pH and temperature

(empirical relationships between soil pH and redox potential have been developed across a variety of soil types and a correction factor of -59 mV per unit of pH change has been proposed, but this correction is not necessarily applicable to soils with high pH buffering capacity [Sparks, 2003]). 2) the spatial heterogeneity of soils means there may be nearby microsites within the soil structure which are at a very different potential to the point of measurement [*Parkin*, 1987; *Teh and Silver*, 2006]. Both of these factors makes it difficult to define exact Eh thresholds at which any particular biogeochemical reaction will or will not occur, but redox potentials can be used to examine the spatial and temporal patterns in the degree to which soils are oxidising or reducing, the drivers of those patterns, and the linkages to biogeochemical properties within the system of interest (in this case, permafrost catchments) [*Fiedler and Sommer*, 2000; *Fiedler et al.*, 2007].

Here, we present findings of a study examining how seasonal deepening of the thaw front and changes in hydrological conditions influence soil redox potentials and the concentrations of methane in the soils and stream of an Arctic headwater catchment. The overall aim of the study was to understand the role of soil redox dynamics in determining conditions for methanogenesis, and the subsequent potential for delivery of dissolved methane in active layer soil water from soils to stream waters. We address the following specific questions: 1) how do redox conditions in hillslope soils vary through the thaw season as the active layer deepens? 2) to what degree are redox potentials in soils related to soil methane concentrations? and 3) to what extent are changing soil redox conditions linked to in-stream redox dynamics and aquatic methane concentrations? We expect that reducing conditions, which develop in saturated soils above the active layer, are associated with methane generation, and that methane present at depth in hillslope soils adjacent to the stream channel can impact stream water methane concentrations via discharge of active layer soil water.

2 Methods

2.1 Site description

The study was carried out in the Siksik Creek catchment (68°44'54.5" N, 133°29'41.7" W), approximately 55 km north-northeast of Inuvik, NWT, Canada (Fig 1). Siksik Creek is a first-order stream flowing north to south with a total catchment area of 0.94 km^2, and is a tributary of Trail Valley Creek, which flows into the Husky Lakes saltwater regions to the East. The mean elevation of the site is *c*. 80 m above sea level, with approximately 30 m difference in altitude between the stream channel and hill tops. The transect established to measure redox potentials in the soil profile (see Sect. 2.2) was located in the middle of the catchment, with a sub-catchment area of *c.* 0.53 km^2. The transect was located in a mid-catchment position sufficiently far upstream of the pre-established water sampling site to avoid disturbance. Based on observation of the surrounding vegetation and topography, we had no reason to believe the location was atypical in comparison to other nearby mid-catchment positions.

The study catchment is in the continuous permafrost zone of the western Canadian Arctic. Mean air temperatures were -16.7°C for October 2013 to April 2014, and 7.1°C for May to September 2014; similar to the mean monthly temperatures in the region of 7.7°C (± 1.1 σ) from May to September and -20.9°C (± 2.1 σ) from October to April [*Teare*, 1998]. Precipitation in 2014 was 277 mm, similar to mean annual precipitation from 1960 to 2005 [*Marsh* et al., 2002]. The freshet, derived from Spring snowmelt, dominates the hydrology of the area and comprises *c.* 90% of annual flow [*Quinton and Marsh*, 1999]. The freshet commenced in late May in 2014, following an eight-month snow covered season, with deep snow beds remaining until mid-June.

Soils in the catchment are organic-rich cryosols, 0.05-0.5 m thick, overlying a 1m thick Quaternary Pleistocene till layer which is underlain by unconsolidated chert, quartzitic

sandstone and siltstone alluvial gravel of the Tertiary Beaufort Formation [*Rampton*, 1987; *Teare*, 1998]. The till layer is characterised by a heterogeneous hummock-inter hummock morphology (0.4-1 m wide and 0.1-0.4 m high). The inter-hummock areas have deeper organic soils than the hummocks and dominate the hydrological response of the catchment following the freshet [*Quinton and Marsh*, 1998, 1999; *Quinton and Pomeroy*, 2006; *Quinton* et al., 2000]. The streambed is composed of the same till material as in the mineral hummocks, with organic-rich sediment deposits of 0.1 – 0.2 m in the stream channel (Table 1).

The vegetation is characterised by upland heath tundra, with lichens, prostrate *Salix* species, and ericaceous shrubs on the hill tops, and patches of dwarf birch (*Betula glandulosa*) and green alder (*Alnus viridis*) on the hillslopes. Bordering Siksik Creek (up to approx. 1-2 m width) is denser vegetation dominated by tall shrub growth forms including *B. glandulosa,* and *Salix* species; we refer to this area as the riparian zone. The area immediately adjacent to the riparian zone at the bottom of the hillslopes is often without shrubs and has high moss cover, including *Sphagnum* species (we refer to this as "channel bank". Sedges (predominantly *Carex* spp.) are common within the riparian zone and the stream channel. Both stream water and soils in the catchment are low in mineral nutrient concentrations; nitrate -N is below detection limit in Siksik Creek [Dean *et al*. in press] and < 2 μg g^{-1} in soils in green alder dominated vegetation at the same site (L. Street, unpublished data).

2.2 Redox potential measurements

We established a 28 m long transect of 9 sampling points (R1 in the stream channel to R9 furthest from the stream channel) running perpendicularly from the stream channel across the channel bank to a lower-hillslope position within a large east-facing patch of *A. viridis* (Fig 1). Hummock morphology is less well-developed in the lower hillslope and channel bank

areas. Redox potentials were measured using probes following the methods of Vorenhout et al., [2011]. The redox probes were 12 mm in diameter and constructed of fibreglass material with embedded platinum electrodes (Paleoterra, Amsterdam, Netherlands). The probes were inserted vertically into the soil; six probes were 0.4 m long in total and had redox electrodes at 0.02 m, 0.12 m and 0.22 m from the probe tip, three probes were 0.6 m long, with redox sensors at 0.02 m, 0.22 m, 0.32 m and 0.42 m from the tip. We inserted the probes in stages over the course of the thaw season as the permafrost thaw front deepened, such that electrodes were positioned at 0.1 m, 0.2 m and 0.3 m depth for the shorter probes, and 0.1 m, 0.2 m, 0.3 m and 0.5 m depth for the longer probes. This meant that the depth of measurement in the soil profile was kept constant (to the nearest cm), even though the specific electrode positioned at a particular depth changed at intervals during the season. The probe in the centre of the stream channel was positioned such that one electrode measured the redox potential of the stream water 0.1 m above the stream bed surface. We did not install the probes the previous winter to avoid potential damage due to freeze-thaw effects and frost heave; they were instead installed on the 12th June, early in the growing season, with measurements starting immediately. We used a Ag/AgCl reference electrode positioned at the mid-point of the transect at a depth of 0.2 m. This electrode is designed for permanent installation in soils and consists of a stable Ag/AgCl element surrounded by a solid electrolyte. A porous ceramic plug allows contact between the electrolyte and the soil (Type WE200, Silvion, Grantham, UK).

Redox potentials and temperatures were logged using a datalogger (CR800, Campbell Scientific, Logan, USA) connected to a 32 channel relay multiplexer (AM16/32B, Campbell Scientific, Logan, UK). Measurements were taken and stored every 10 minutes. Electron flow between electrodes during a redox potential measurement can result in drift effects as the proportion of oxidised and reduced species changes via reaction with the surface of the probe.

However, if high measurement resistances are used current flow is extremely low, and these effects can be can be minimised The input resistance of the datalogger was 20 GΩ, sufficient to prevent significant drift effects on soil redox potential when used in conjunction with a multiplexer, which maintains an open circuitry except during the period of measurement [*Rabenhorst* et al., 2009]. Data are expressed relative to a standard hydrogen electrode, but not corrected for temperature and pH. Eh is positive and high in oxidizing systems and low or negative in reducing conditions, and would be expected to decrease as pH increases. As detailed above, it is impossible to define an exact redox potential threshold at which methanogenesis will occur, but the range 0 to +300 mV is usually defined as "moderately reducing" conditions, in that electron acceptors other than O_2 begin to be utilised [*Fiedler et al.*, 2007]. Within this range we choose to define "reducing conditions" as Eh < +200mV on the basis that [*Yu et al.*, 2007] found the methane compensation point in soil (production = consumption) to be around + 400 mV at pH 7, which is roughly equivalent to +240 mV at the minimum pH for our system. In reality, however, there is a gradient between "oxidising" and "reducing" conditions in soils.

Redox sensors can function reliably in unsaturated soils, as long as adequate contact is maintained between the probe and the soil, and this is possible as long as soils are sufficiently moist. Van Bochove *et al*. [2002] demonstrate reliable redox measurements for soils with volumetric water content (VWC) between 0.20 $m^3\ m^{-3}$ and 0.29 $m^3\ m^{-3}$. We monitored the VWC of soils at 0.05 m depth at a nearby location on the stream bank (approximately 10 m from the redox probe measurements) using a HOBO ECH_2O soil moisture probe (Onset Inc, Pocasset,MA, USA). Data were recorded every 10 min using HOBO Micro-Station data loggers (Onset Inc). VWC measured by the moisture probes varied between ~ 0.2 and 0.5 $m^3\ m^{-3}$ over the measurement period (Supplementary Fig. S2).

We tested the variability between the electrodes prior to installation by placing the probes in tap water. The tap water in the Inuvik area, where this testing was carried out, is sourced from a local lake and is therefore similar to soil solution in that it contains a complex mix of dilute redox couples at low concentrations. Our primary aim was to check the probes were functioning as expected, and to quantify consistency between probes. For the reasons outlined above, it is difficult to standardise redox potential measurements, so the absolute value of redox potential is not of primary importance. The average reading across all electrodes in tap water was +277 mV ± 7 σ which is a typical value for tap water [*Goncharuk et al.*, 2010] and the variability between probes was small in comparison to previously published data [*Fiedler et al.*, 2007]. (Supplementary Fig S1). The electrode at 0.32 m from the tip on probe R1 was an outlier in this test, and was also unresponsive to reducing conditions in the field (as indicated by the electrodes both above and below on the same probe) so data from this electrode was excluded from further analysis.

2.3 Soil greenhouse gas measurements

To measure soil methane concentrations, we used soil gas sampling probes (following the protocol of [*Dinsmore* et al., 2009]). which involved collecting gas phase samples from soils through a water-impermeable membrane. This allowed us to quantify the gaseous concentration of methane in equilibrium with the surrounding soil pore water. We chose this method so that we could collect data from both saturated and unsaturated soils along the length and depth of the transect, including stream sediments. Since the volume of water that the gas probe is in equilibrium with is not known, it is inappropriate to represent the value as an aqueous concentration, and we express the soil gas data as ppmv. The soil gas probes were constructed of 6 mm OD steel tubing (Swagelok, Solon, USA) and were inserted into the soil at depths of 0.1, 0.2, and 0.3 m, within 1 m distance of the redox probes. We inserted gas

sampling probes to the maximum possible depth as the thaw front deepened (from a minimum of 0.08 m at the beginning of the thaw season to max. 0.68 m at the end), until probes were situated at the target depths. We installed extra gas probes and sampled from the deepest possible depths (up to 0.68 m) at three locations: in the middle of the stream channel (near R1), on the edge of the stream channel (near R2) and at the uppermost position on the hillslope (near R9). The soil sampling probes were sealed at the bottom, but had openings at a distance of 2.5 cm from the end of the probe which were covered by a 5 cm length of gas permeable/water impermeable membrane (ACCUREL® PP V8/2 HF), which allows gases to diffuse into the tube without water ingress. The ACCUREL membrane was sealed to the probe using rubber paint (Plasti Dip®, Petersfield, UK), and the entire tube covered with white heat-shrink rubber tubing to minimise heat absorption by metal parts exposed to solar radiation. Prior to each sampling, a volume of air equal to the approximate internal volume of the probe was purged to the atmosphere. Suction was then applied to the tube using a 60-ml syringe for 48hr (72 hr in September) then 20 ml of sample was injected into a 12 ml pre-evacuated gas-tight borosilicate Exetainer® vial (Labco, UK) . Where less than a 20 ml volume of gas was collected over the sampling period, the remaining volume was made up to 20 ml in the laboratory using standard gas of known CO_2 and methane concentration, and sample concentrations calculated after analysis by mass balance:

$$C_S = \frac{C_M \times 20\ ml - C_D \times V_D}{V_S} \qquad \text{Eq. (1)}$$

Where C is the concentration of either CO_2 or methane, and V the volume of respective gas fractions. Subscripts denote sample (S), dilution gas (D) and measured (M) concentrations and volumes, respectively.

We collected 184 gas samples in total, of which 112 contained more than 4 ml of sample. The samples were analysed for CO_2 and methane concentrations using gas chromatography (Hewlett-Packard, HP5890, Series II gas chromatograph, fitted with two 2-m Hayes Sep Q columns (80-100 mesh) in series, and including a CO_2 methanisation catalyst and flame ionization detector) at the University of Stirling, UK.

2.4 Stream greenhouse gas concentrations.

Dissolved methane and CO_2 gas samples (n = 8) were collected in the stream *ca*. 30 m downstream of the transect using the headspace technique [*Kling* et al., 1992; *Dinsmore* et al., 2013]. A 40 ml water sample was equilibrated with a 20 ml headspace of ambient air (collected from between 2 and 10 cm water depth) in a 60 ml syringe at natural stream temperature by shaking the syringe for 1 min vigorously underwater at the sampling point. Sampling depth was noted and used to calculate total (air plus water) system pressure, along with *in situ* field parameters (pH, electrical conductivity – EC, and temperature) using Hanna Instruments® HI-9033 and HI-9124 meters. The equilibrated headspace was then injected into a 12 ml pre-evacuated Exetainer® vial. Multiple ambient samples were collected and stored in Exetainer® tubes during sampling days. Both headspace and ambient samples were analysed at the Centre for Ecology and Hydrology (CEH Edinburgh, UK) on an HP5890 Series II gas chromatograph (Hewlett–Packard) with flame ionization detector and attached methaniser. Detection limits for methane were 84 ppbv. Henry's Law was then used to calculate concentrations of CO_2 and methane dissolved in the stream water from the headspace and ambient concentrations [e.g. *Hope* et al., 1995]. Stream CO_2 and methane concentrations on one occasion (22 July) were not measured so were estimated from the relationship between CO_2 and methane concentrations ($\mu g\ l^{-1}$) and DOC at the same location (including 4 samples taken in early June and mid-September; data not shown) (methane

versus DOC, $R^2 = 0.62$, $p < 0.01$, , n = 10). Surface water samples for dissolved organic C (DOC) were collected using a 60 ml syringe from approximately 5 cm depth in the water column and the sample injected through 0.45 μm Millipore syringe-driven filters and stored without headspace in 30 or 60 ml bottles that were first rinsed with the filtered sample. Samples were kept cool (< 6°C) and dark prior to analysis. The filtrate was analysed for DOC concentration at CEH Edinburgh on a PPM LABTOC Analyser (detection range of 0.1–4000 mg l^{-1}); concentrations were calculated based on a three-point calibration curve with a maximum of 50 mg C l^{-1}. GHG concentrations are expressed as μg l^{-1} (CH_4 or CO_2) or excess partial pressure ($epCH_4$), defined as the partial pressure of methane in solution divided by the partial pressure of methane in the atmosphere.

2.5 Other field measurements

We measured shallow groundwater levels during the thaw season using 2.5 cm diameter PVC piezometers at 5 positions (within 1m of R3, R4, R6, R7 & R9), as well as the depth of the thaw front at each transect position, for each gas sampling event. Soil pH was also determined for each redox probe position and depth in the laboratory on field-moist soil (2:1 w/w soil: de-ionised water) collected using a 2.5 cm gauge corer.

Daily precipitation data were obtained from the nearby Environment Canada weather station approx.. 320 m from our sampling location (Station ID: 220N005; 68°44'46.8" N, 133°30'06.4" W).

2.6 Data analysis

To test relationships between soil methane concentrations and redox conditions in the active layer, candidate models were compared using the leaps (v2.9) package in R (v3.1.2) [*R Development Core Team*, 2009]. This analysis involved an exhaustive search of all possible

linear models including any or all of the following seven explanatory variables: soil depth (m), redox potential at time of sampling (Eh, mV), soil temperature (ºC), active layer depth (m), water table depth (m), number of days (since soil thaw) that Eh < 200mV (days), and date (DOY; day of year).

The best-supported linear model was selected based on Akaike Information Criterion AIC, a criterion allowing model selection based on a trade-off between goodness of fit and model complexity which penalises over-fitting. Methane concentration data were $\log_{10}$ transformed prior to analysis.

To examine potential coupling between hillslope soils and stream water methane concentrations, Pearson correlations were calculated between stream water methane concentrations and hillslope soil methane concentrations at each soil depth and hillslope position. We had limited data from stream sediments at 0.3 m < depth < 0.5 m so data from these depths were grouped into a single depth category.

3 Results

3.1 Site conditions

Weather conditions in July 2014 were generally warmer and drier than in August, with maximum daily air temperatures in July often exceeding 20°C (Fig 2a). There was a change in weather conditions from the end of July, with cooler air temperatures approaching freezing overnight. Stream temperatures also dropped from the end of July (mean daily temperature for July 11.4°C), and were generally lower in August (mean daily temperature 7.3°C). The reduction in air temperature at the end of July was accompanied by an increase in precipitation and stream discharge (Fig 2b); average daily stream discharge for July was 1.9 mm day^{-1}, and for August 3.9 mm day^{-1}. The largest single rain event occurred on 24th August at approx. 4am, when 29 mm of precipitation fell over 24hr, equivalent to 50 % of the total precipitation for July (Fig 2b). The extent of the saturated soil zone above the frost table was also greater in August/September (varying from 0 m at R3 to a maximum of *c*. 0.38 m at R7) than in July (0 m at R3 to *c*. 0.21 m at R7) (Table 1).

Thaw depth at the beginning of the measurement period was 0.10 – 0.19 m across the hillslope and channel bank, and 0.35 m in the stream channel. Thaw depths increased to a maximum value of 0.57 m on the hillslope (at R7) and 0.81 m in the stream channel (R1) by September (Table 1). The shallowest thaw depths by the end of the measurement period were at R3 (0.35 m) and R4 (0.41 m). The depth of the soil organic horizon was on average 0.16 m for R5-R9, but deeper at R3 and R4 on the lower hillslope where the depth of organic soil exceeded the maximum thaw depth. Sediments in the stream were highly organic to a depth of 0.1 – 0.2 m, but a dense root mat extended to depths > 0.5 m in the centre of the stream channel. Soil pH varied between 4.6 – 5.7; there was no clear pH trend with soil depth (Table 1).

3.2 Redox dynamics in hillslope soils

Soil redox potentials (Eh) were greater than +400 mV at 0.1 m and 0.2 m depth across the hillslope and channel bank (R3-R9) for the duration of the growing season (Fig 3, Fig 4). There was a negative trend in Eh through time at the hillslope positions (R5-R9) at 0.3 m depth, and Eh values fell below +200 mV from the beginning of August onwards at R6 and R7. Eh < 200 mV was also recorded at 0.5 m at R9 in early September (Fig 4). The lowest Eh values recorded in the hillslope soils were at R7 where Eh was < 0 mV from 2nd August onwards (Fig 3a). On the channel bank at R3 and R4, Eh was > +600 mV at all profile depths throughout the thaw season (Fig 4), though data for R4 at 0.3 m were only available from the end of August (Fig 3b) because active layer depths were shallower at this position (Table 1). There was a simultaneous increase in Eh from approx. +400 mV to +600 mV on 25th August around 0200hr at R6 (0.2 m) and R9 (0.3 m), which occurred following the large rain event on 24th August and also coincided with a significant increase in stream discharge (Fig 2b). Eh at these positions then began to decrease again after approximately three days (Fig 3a).

3.3 Redox dynamics in stream water and channel sediments

Redox potential in the stream water and shallow sediments (0.1 m depth) varied between approximately +600 mV and -100 mV over the course of the thaw season (Fig 3c). In mid-July there was a period during which Eh was significantly lower in the mid-channel stream water and shallow sediments (R1) than during the rest of the measurement period, eventually reaching negative values on 18th July (Fig 3c). Stream water and shallow sediment redox potentials then returned to values around + 600mV in early August, but Eh in the stream water recovered approximately 3.5 days earlier than in the sediment. On 24th August at approximately 0900, Eh in the stream sediments at 0.1 m decreased from approximately +650 mV to + 350 mV then recovered over the next three to four days (Fig 3c). This decrease in Eh

in the shallow sediments also occurred following the large precipitation event and subsequent spike in stream discharge, which began on the 24th August. Eh values for the deeper stream sediments (0.2 m and deeper), both in the mid-channel (R1) and channel edge (R2), remained between -100 and +100 mV for the entire measurement period (Fig 3c, Fig 4).

3.4 Greenhouse gas concentrations in hillslope soils and channel sediments

Average methane concentrations (in parts per million by volume; ppmv, subsequently denoted ppm) in upper organic hillslope soils (at 0.1 m depth) varied between 1.2 and 34 ppm. The highest methane concentrations at 10 cm depth were measured on 30th August at R6 (17 ppm) and R7 (3.3 ppm) and on 3rd September at R6 (34 ppm) and R7 (3.1 ppm) (Fig 5). At all other locations on the hillslope soil methane at 0.1 m depth was on average 2.1 ± 0.05 ppm (comparable to atmospheric concentrations) over the duration of the thaw season. In general, soil methane concentrations increased over time, and with depth in the profile (Fig 5). The exception was on the lower hillslope at R3, where average concentrations at 0.2 m depth (1.3 ± 0.15 ppm) were consistently lower than at 0.1 m (2.1 ± 0.02 ppm) and 0.3 m depth (7.9 ± 2.8 ppm). Methane concentrations in the stream bed sediments were several orders of magnitude higher than those in hillslope soils (Fig 5, Fig 6a). At ≥ 0.2 m depth methane concentrations in the stream sediments varied between 15 and 160,168 ppm. The highest concentration of 160,168 ppm (16.2 % by volume) was measured on 30th August at R2 at 0.5 m depth (Fig 5c). At 0.1 m depth methane concentrations in the stream sediments varied between 1.5 – 54 ppm (Fig 5). CO_2 concentrations varied between 3628 and 528,000 ppm in the stream sediments, and 483 and 154,000 ppm across the hillslope (Supplementary Fig S3).

The best supported model of soil and sediment methane concentrations included four parameters; measurement depth, water table position, thaw depth, and number of days Eh <

+200 mV. This model was able to explain 84 % of the variability in log(CH_4 concentration) (Table 2). An identical model using redox potential immediately prior to measurement rather than the number of days Eh < 200 mV explained 76 % of the variability in measured log(CH_4 concentration).

3.5 Aquatic methane concentrations

Stream water methane concentrations varied between 1.4 and 11.7 μg l^{-1} (50 – 490 μatm) between mid-June and early September (Fig 7a). These concentrations correspond to epCH_4 values of approximately 28 – 234. The highest recorded stream water methane concentrations occurred between 14th and 16th July when stream discharge was low. The lowest stream water methane concentrations occurred in late August and September (Fig 7a). All the stream water samples were taken during periods when redox potential in the water column was greater than + 300 mV (Fig 7a) and there was no correlation between stream water redox potential and stream water methane concentrations.

Fig 7b shows a 'heat map' of the strength of correlation between soil methane concentrations, and stream water methane concentrations through time, for each distance from the stream and depth in the soil profile. There was some evidence of a positive association between stream water and soil methane concentrations at 0.2 m depth on the channel bank (R3), but in general methane concentrations were negatively correlated with soil methane concentrations through time. These correlations were strongest in the mid-hillslope positions (Fig 7b).

4 Discussion

4.1 How do redox conditions in hillslope soils vary through the thaw season as the active layer deepens?

Redox potentials varied between -200 and +700 mV, a typical range for soils under natural conditions [*Yu* et al., 2007]. On the channel bank within 5 m of the stream, the organic horizon was deeper and the maximum thaw depth shallower than elsewhere on the transect; as a result the active layer soil profile consisted only of organic material. The expectation might be that these highly organic soils would more quickly generate reducing conditions [*Ponnamperuma*, 1972], however at these locations redox potentials were oxidising at all depths because there was no persistent saturated soil zone above the permafrost table. The underlying topography of the permafrost, or the greater hydraulic conductivity of the organic soil, presumably promoted rapid drainage at this location (Fig 8). At distances greater than 5 m from the stream, saturated soils of 0.1 m to 0.3 m depth overlay the permafrost table for most of the thaw season; however, even where soils were saturated it took time for reducing conditions to develop. The only hillslope locations where soils became strongly reducing were at R6, R7 and R9, but at these locations redox potential did decrease to less than +200 mV by the end of the thaw season.

By contrast, redox conditions at depth in the stream channel were strongly reducing from the beginning of the measurement period in mid-June. While it is possible that reducing conditions had developed rapidly early in the spring before measurements began, considering the slow trajectory of change in Eh further upslope, and the very high concentrations of methane observed early in the season, it is more likely that redox conditions remain reducing all year round at depth beneath the stream. Biological activity can continue in active layer soils over the winter [*Hultman* et al., 2015], and may be significant beneath the stream bed

where temperatures can remain close to 0 °C [*Mikan* et al., 2002] due to heat flux associated with running water [*Bradford* et al., 2005]. Considering also that large quantities of root material were present at depth below the channel, providing a potential carbon substrate, year round biological activity probably contributes to maintenance of reducing conditions throughout the year in the deeper stream sediments.

A simultaneous increase in redox potential of ~200 mV in soils at 20 cm depth at R6 and R7, and at 30 cm depth at R9, coincided with a major rain event on the 24th August. Shifts in redox potential of this magnitude have previously been recorded in upland soils in response to precipitation events [*Mitchell and Branfireun*, 2005]. This increase may be caused by reduced groundwater being displaced by infiltrating oxygenated rain water, or by more oxygenated subsurface water through lateral flow from upslope. There was no response deeper in the soil profile at R6 and R7 to the same rain event, suggesting that downwards vertical flow in these locations was impeded or that the majority of the rainfall flowed overland or as shallow subsurface flow rather than in the deeper subsurface. This is consistent with previous work at the same site which has shown that near-surface peat soils provide less resistance to water movement than deeper layers, resulting in lateral water flow through near-surface soils [*Quinton* et al., 2000].

The presence of oxygenated conditions in the shallower stream sediments and water column showed that negative redox conditions can persist in the thaw bulb – thawed soils beneath the hyporheic zone [*Greenwald* et al., 2008] – probably because of limited exchange between the sediments and stream waters (Fig 8). This was true even under storm flow conditions in late summer – redox potentials did not respond in the deeper sediments to the rain event which occurred on the 24th August. The decrease in redox potential in the shallower stream sediments at this time may indicate that, under high flow conditions, there was an increase in

the level of the less oxygenated groundwater below the stream bed i.e. subsurface water was discharged towards the streambed as hillslope water was displaced, leading to a reduction in redox potential in the shallower sediments. An alternative explanation is that the upper hillslope becomes hydrologically connected and lateral flow from upslope soils into shallow organic sediments within the hyporheic zone temporarily impacts stream redox conditions; early stormflow is probably composed mainly of displaced pre-event soil water on the basis of evidence from other peat-dominated catchments [*Tetzlaff* et al., 2015].

4.2 How are redox potentials in hillslope soils related to soil methane concentrations?

We observed elevated methane concentrations at depth in the hillslope soil profiles, with concentrations generally increasing over time through the season, as expected with the development of more negative redox conditions [*Fiedler* et al., 2007; *Yu* et al., 2007]. There was a clear positive relationship between methane concentrations and the amount of time for which redox potential in the soil or sediment was less than +200 mV; the duration of time for which reducing conditions were present was a better predictor of methane concentrations than instantaneous redox conditions at the time of measurement. This could be due to the build-up of methane over time in the soil, but could also reflect time lags inherent in the growth of methanogenic microbial communities once electrochemical conditions are favourable [*Lipson* et al., 2015] or the depletion of alternative electron acceptors such as NO_3^-, Fe(III) and SO_4^{2-} [*Peters and Conrad*, 1996]. Nitrate is unlikely to play a major role due to the low concentrations of nitrate found in soils at this site, even in vegetation dominated by *A. viridis* which is an N fixer [L. Street, unpublished data]. Recent evidence also suggests that organic matter can act as a terminal electron acceptor in temporarily anoxic environments which may also contribute to time lags in CH_4 formation [*Klüpfel et al.*, 2014]. We found high concentrations of methane in the deep stream channel sediments throughout the thaw period.

It is likely then that these high concentrations at depth in the early thaw season reflect methane production from previous years, including overwinter methane production [*Zimov* et al., 1997], concentrations having built up due to slow rates of transport through fine sediments, either via diffusion or ebullition [*Crawford* et al., 2014b].

As expected, negative redox potentials and enriched methane concentrations deeper in the soil profile indicate that the saturated zone above the permafrost table does provide conditions suitable for methanogenesis. Methane generation at depth in the soil profile does not necessarily result in a net methane efflux from the soil surface, as some or all of this methane may be oxidised in the surface layers [*Segers*, 1998, *Whalen* et al.,1990], which we demonstrate had consistently oxidised redox potentials throughout the thaw season. The scope of this study did not include quantifying net terrestrial surface methane fluxes, but we did find evidence of significant methanotrophy within the organic soils on the channel bank, where concentrations of methane were below ambient atmospheric concentrations at 20 cm soil depth despite elevated concentrations in deeper soils. The stream surface does act as a net source to the atmosphere, however, as methane concentrations in the stream were consistently supersaturated with respect to atmospheric concentrations.

4.3 To what extent do changing active layer soil conditions influence in-stream redox potential and aquatic methane concentrations?

We found negative correlations between hillslope soil methane concentrations and the concentration of methane in the stream water. Negative correlations were a result of increases in methane concentrations in hillslope soils over time as negative redox potentials developed, while methane concentrations in stream water peaked in July, probably as a result of low discharge rates and warmer temperatures. Instantaneous stream water methane concentrations and hillslope soil methane concentrations were not correlated in this context, and in contrast

539 to Paytan et al., [2015] groundwater discharge from the active layer did not appear to result in
540 increased aquatic methane concentrations. The stream methane data are limited, however, and
541 there may be time lags involved which were not possible to test due to a limited number of
542 data points.

543 Methane concentrations in the deep stream bed sediments were several orders of magnitude
544 higher than in hillslope soils. This raises the possibility that the processes determining
545 methane transport from deeper, mineral stream sediments may be more important than lateral
546 methane transport from hillslope soils in determining stream methane concentrations and
547 efflux (Fig 8). These processes will include rates of diffusion and ebullition [*Wik* et al.,
548 2014], and plant-mediated transport, as well as rates of methanotrophy in oxidised sediments
549 or surface waters [*Schimel*, 1995]. Low stream discharge rates did result in strongly reducing
550 redox conditions in the stream water for a week long period in July; this could potentially
551 have dramatically reduced in-stream methane oxidation, and aquatic methane concentrations
552 and surface fluxes may therefore have been higher. Unfortunately, our field campaigns did
553 not coincide with the period when stream redox potentials were lowest, so we are unable to
554 draw strong conclusions on the influence of stream redox conditions on stream water
555 methane concentrations.

556 Spatial variability in the processes linking soil redox conditions and stream water
557 biogeochemistry is likely to be high. Biogenic methane production in soils is highly spatially
558 variable [*Moore et al.*, 1990; *Wachinger et al.*, 2000], and the processes mediating the
559 transport of dissolved gases between the aquatic and terrestrial system are also likely vary
560 spatially along the length of the stream [*Waddington and Roulet*, 1997; *Hope et al.*, 2004;
561 *Crawford et al.*, 2013]. We had no reason to believe that the transect was atypical, as it was
562 situated between a common landscape unit (Alder shrub) and the stream bank, but we cannot

563 generalise our results to the whole catchment on the basis of this single transect. . The
564 subcatchment of the transect was topographically linear, and while we find no evidence
565 supporting the importance of terrestrial-aquatic methane transfer pathways in this particular
566 case, this does not mean that these processes are never important. Concave subcatchment
567 topographies for example may lead to increased biogeochemical influences from upslope
568 [*Mitchell et al*. 2009]. However, our data do show consistent patterns in soil redox potential
569 both through time and with soil (or stream) profile position, and we also show that redox
570 conditions are strongly related to methane accumulation in soils. This study, therefore,
571 provides a basis for further work which can test landscape-scale methane dynamics in more
572 detail. For example, the use of an expanded grid or network of continuously deployed redox
573 probes could be used to interpolate spatial and temporal patterns in methane concentrations
574 over larger scales. This kind of data is currently extremely challenging to obtain because of
575 the need for intensive manual sampling in difficult and (often) remote terrain, but would
576 allow for a much more comprehensive analysis of methane source areas, and the potential for
577 lateral transfers of methane at the catchment scale.

578 **4.4 Implications for catchment scale methane budgets**

579 It was beyond the scope of this study to quantify methane evasion fluxes from along the
580 length of Siksik creek. However, we are able to provide context in terms of the aquatic
581 contributions to methane fluxes at the catchment scale, based on the limited data available for
582 other permafrost stream systems. Crawford *et al.* [2013] measured average fluxes during the
583 open water season of between 0 – 80.5 mg CH_4 m^{-2} d^{-1} for streams within a headwater
584 catchment of the Yukon River Basin, and estimate efflux from the stream network to account
585 for up to ~10 % of the terrestrial methane source strength. Measured $epCH_4$ values for
586 streams in Crawford *et al.* [2013] varied between approx. 0.6 – 7, which are low compared to
587 values of 28 – 234 in this study. Flessa *et al.* [2008] report $epCH_4$ values between 54 – 1290

588 for streams at the forest-tundra ecotone in northern Siberia, but do not quantify evasion
589 fluxes. In a catchment with sporadic permafrost in northern Sweden, *Lundin et al.*, [2013]
590 report epCH4 values between 54 – 1290 and corresponding mean methane fluxes from the
591 stream surface which were high (253 mg CH_4 m^{-2} d^{-1}) compared to diffusive fluxes from
592 lakes (12 mg CH_4 m^{-2} d^{-1}). Per unit catchment area, streams made an equivalent contribution
593 to methane release as lakes, not including ebullition fluxes (around 0.1 g CH_4 m^{-2} yr^{-1}). We
594 did not quantify terrestrial surface methane fluxes for the wider Siksik creek catchment, but
595 it is likely that for a significant fraction of the land surface corresponding to dwarf
596 shrub/lichen dominated tundra, soils act as a small net sink for methane over the growing
597 season (O. Sonnentag, pers. comm.).

598 **4.5 Summary and wider implications**

599 Figure 8 presents a conceptual model of the processes linking hillslope, redox conditions, and
600 methane concentrations in soils and streams within the headwater catchment studied.
601 Reducing conditions develop in active layer hillslope soils over the course of the growing
602 season, but soil saturation conditions determine where and when reducing conditions
603 develop (1). In this context, a zone of normally unsaturated organic soils exists at the edge of
604 the stream channel (2) in which methane oxidation results in soil methane concentrations
605 which are below atmospheric concentrations. Redox conditions in stream water and shallow
606 stream sediments are usually oxidising, but during periods of low flow can decrease to
607 become strongly reducing. We also find evidence that precipitation events can influence both
608 soil and stream redox conditions but only to a limited depth. High methane concentrations
609 develop in stream sediments beneath the zone of hyporheic exchange (3). We find no
610 evidence that increasing methane concentrations in the hillslope active layer during the
611 growing season have an impact on methane concentrations in the stream water. (4). Ebullition

612 or diffusion from deeper stream sediments, may therefore be more important than hillslope
613 redox dynamics in determining aquatic methane fluxes under future climatic conditions. To
614 our knowledge, this study is the first to explicitly examine the linkages between redox
615 conditions in hillslope permafrost soils and headwater streams, and therefore provides
616 important process-based information for an improved understanding of methane
617 biogeochemistry under changing hydroclimatic regimes in a warming Arctic.

618 **Acknowledgements**

619 This work was funded by NERC grants NE/K000284/1 (PA Wookey), NE/K000225/1 (R
620 Baxter), NE/K000217/1 (MF Billett) and NE/K000268/1 (D Tetzlaff) as part of the NERC
621 Arctic Research Programme. We would like to thank the staff at the Aurora Research
622 Institute, as well as Prof Philip Marsh and Prof Oliver Sonnentag, for providing logistical
623 support. We also thank Philip Marsh and Oliver Sonnentag for assisting with access to long-
624 term meteorological and hydrological information. Daily precipitation data for Trail Valley
625 Creek are available from Environment Canada at http://climate.weather.gc.ca/. Data from the
626 present study will be made available via the UK Environmental Information Data Centre
627 (EIDC). Requests for access to the data should be directed to Prof Philip Wookey
628 (p.a.wookey@hw.ac.uk). We thank Ian Washbourne and Gwen Lancashire for their
629 assistance with the fieldwork. We also thank three anonymous reviewers for their helpful
630 suggestions in improving the manuscript.

631 **References**

632 Bastviken, D., L. J. Tranvik, J. Downing, P. M. Crill, and A. Enrich-Prast (2011), Freshwater
633 Methane Emissions Offset the Continental Carbon Sink, *Science (80-.).*, *331*, 50,
634 doi:10.1126/science.1196808.

635 Baulch, H. M., P. J. Dillon, R. Maranger, and S. L. Schiff (2011), Diffusive and ebullitive
636 transport of methane and nitrous oxide from streams: Are bubble-mediated fluxes
637 important?, *J. Geophys. Res. Biogeosciences*, *116*(4), doi:10.1029/2011JG001656.

638 Billett, M. F., and T. R. Moore (2008), Supersaturation and evasion of CO_2 and CH_4 in
639 surface waters at Mer Bleue peatland, Canada, *Hydrol. Process.*, *22*(October 2007),
640 2044–2054, doi:10.1002/hyp.

641 Bradford, J. H., J. P. McNamara, W. Bowden, and M. N. Gooseff (2005), Measuring thaw
642 depth beneath peat-lined arctic streams using ground-penetrating radar, *Hydrol.*
643 *Process.*, *19*(14), 2689–2699, doi:10.1002/hyp.5781.

644 Crawford, J. T., R. G. Striegl, K. P. Wickland, M. M. Dornblaser, and E. H. Stanley (2013),
645 Emissions of carbon dioxide and methane from a headwater stream network of interior
646 Alaska, *J. Geophys. Res. Biogeosciences*, *118*(2), 482–494, doi:10.1002/jgrg.20034.

647 Crawford, J. T., N. R. Lottig, E. H. Stanley, J. F. Walker, P. C. Hanson, J. C. Finlay, and R.
648 G. Striegl (2014a), CO_2 and CH_4 emission from stream in a lake-rich landscape:
649 Patterns, controls, and regional significance, *Global Biogeochem. Cycles*, 197–210,
650 doi:10.1002/2013GB004661.

651 Crawford, J. T., E. H. Stanley, S. A. Spawn, J. C. Finlay, L. C. Loken, and R. G. Striegl
652 (2014b), Ebullitive methane emissions from oxygenated wetland streams, *Glob. Chang.*
653 *Biol.*, *1*, 3408–3422, doi:10.1111/gcb.12614.

654 Dean, J.F., Billett, M.F., Dinsmore K.J., Lessels, J. Street L.E, Washbourne, I., Subke, J.A.,
655 Tetzlaff, D., Baxter, R. and Wookey, P.A. (in press), Biogeochemistry of “pristine”
656 freshwater stream and lake systems in the western Canadian Arctic, *Biogeochem*.

657 Dinsmore, K. J., M. F. Billett, and T. R. Moore (2009), Transfer of carbon dioxide and
658 methane through the soil-water-atmosphere system at Mer Bleue peatland , Canada,

659 *Hydrol. Process.*, *341*(November 2008), 330–341, doi:10.1002/hyp.

660 Fiedler, S., and M. Sommer (2000), Methane emissions, groundwater levels and redox
661 potentials of common wetland soils in a temperate-humid climate, *Global Biogeochem.*
662 *Cycles*, *14*(4), 1081, doi:10.1029/1999GB001255.

663 Fiedler, S., M. J. Vepraskas, and J. L. Richardson (2007), *Soil Redox Potential: Importance,*
664 *Field Measurements, and Observations*, Elsevier Masson SAS.

665 Flessa, H., A. Rodionov, G. Guggenberger, H. Fuchs, P. Magdon, O. Shibistova, G.
666 Zrazhevskaya, N. Mikheyeva, O. A. Kasansky, and C. Blodau (2008), Landscape
667 controls of CH_4 fluxes in a catchment of the forest tundra ecotone in northern Siberia,
668 *Glob. Chang. Biol.*, *14*(9), 2040–2056, doi:10.1111/j.1365-2486.2008.01633.x.

669 Goncharuk, V. V., V. A. Bagrii, L. A. Mel'nik, R. D. Chebotareva, and S. Y. Bashtan (2010),
670 The use of redox potential in water treatment processes, *J. Water Chem. Technol.*, *32*(1),
671 1–9, doi:10.3103/S1063455X10010017.

672 Greenwald, M. J., W. B. Bowden, M. N. Gooseff, J. P. Zarnetske, J. P. McNamara, J. H.
673 Bradford, and T. R. Brosten (2008), Hyporheic exchange and water chemistry of two
674 arctic tundra streams of contrasting geomorphology, *J. Geophys. Res. Biogeosciences*,
675 *113*(G2), n/a–n/a, doi:10.1029/2007JG000549.

676 Grundl, T. (1994), A review of the current understanding of redox capacity in natural,
677 disequilibrium systems, *Chemosphere*, *28*(3), 613–626, doi:10.1016/0045-
678 6535(94)90303-4.

679 Hall, S. J., W. H. McDowell, and W. L. Silver (2012), When Wet Gets Wetter: Decoupling of
680 Moisture, Redox Biogeochemistry, and Greenhouse Gas Fluxes in a Humid Tropical
681 Forest Soil, *Ecosystems*, *16*(4), 576–589, doi:10.1007/s10021-012-9631-2.

682 Hershey, A. E., R. M. Northington, J. Hart-Smith, M. Bostick, and S. C. Whalen (2015),

683 Methane efflux and oxidation, and use of methane-derived carbon by larval
684 Chironomini, in arctic lake sediments, *Limnol. Oceanogr.*, *60*(1), 276–285,
685 doi:10.1002/lno.10023.

686 Hope, D., S. M. Palmer, M. F. Billett, and J. J. C. Dawson (2004), Variations in dissolved CO
687 2 and CH 4 in a first-order stream and catchment : an investigation of soil – stream
688 linkages, , *3275*(January), 3255–3275, doi:10.1002/hyp.5657.

689 Hultman, J. et al. (2015), Multi-omics of permafrost, active layer and thermokarst bog soil
690 microbiomes, *Nature*, *521*, 208–212, doi:10.1038/nature14238.

691 Husson, O. (2012), Redox potential (Eh) and pH as drivers of soil/plant/microorganism
692 systems: a transdisciplinary overview pointing to integrative opportunities for
693 agronomy, *Plant Soil*, *362*(1-2), 389–417, doi:10.1007/s11104-012-1429-7.

694 Jones, J. B., and P. J. Mulholland (1998), Methane input and evasion in a hardwood forest
695 stream: Effects of subsurface flow from shallow and deep flowpaths, *Limnol.*
696 *Oceanogr.*, *43*(6), 1243–1250, doi:10.4319/lo.1998.43.6.1243.

697 Kettunen, A., V. Kaitala, A. Lehtinen, A. Lohila, J. Alm, J. Silvola, and P. J. Martikainen
698 (1999), Methane production and oxidation potentials in relation to water table
699 fluctuations in two boreal mires, *Soil Biol. Biochem.*, *31*(12), 1741–1749,
700 doi:10.1016/S0038-0717(99)00093-0.

701 King, J., and W. Reeburgh (2002), A pulse-labeling experiment to determine the contribution
702 of recent plant photosynthates to net methane emission in arctic wet sedge tundra, *Soil*
703 *Biol. Biochem.*, *34*, 173–180.

704 Kling, G., G. Kipphut, and M. Miller (1992), The flux of CO_2 and CH_4 from lakes and rivers
705 in arctic Alaska, *Hydrobiologia*, *240*(1), 23–36, doi:10.1007/BF00013449.

706 Klüpfel, L., A. Piepenbrock, A. Kappler, and M. Sander (2014), Humic substances as fully

707 regenerable electron acceptors in recurrently anoxic environments, *Nat. Geosci.*,
708 *7*(February), 195–200, doi:10.1038/NGEO2084.

709 Knoblauch, C., O. Spott, S. Evgrafova, L. Kutzbach, and E. M. Pfeiffer (2015), Regulation of
710 methane production, oxidation, and emission by vascular plants and bryophytes in ponds
711 of the northeast Siberian polygonal tundra, *J. Geophys. Res. G Biogeosciences*, *120*(12),
712 2525–2541, doi:10.1002/2015JG003053.

713 Lipson, D. A., T. K. Raab, M. Parker, S. T. Kelley, C. J. Brislawn, and J. Jansson (2015),
714 Changes in microbial communities along redox gradients in polygonized Arctic wet
715 tundra soils, *Environ. Microbiol. Rep.*, *7*(4), 649–657, doi:10.1111/1758-2229.12301.

716 Lundin, E. J., R. Giesler, A. Persson, M. S. Thompson, and J. Karlsson (2013), Integrating
717 carbon emissions from lakes and streams in a subarctic catchment, *J. Geophys. Res.*
718 *Biogeosciences*, *118*, n/a–n/a, doi:10.1002/jgrg.20092.

719 Marsh, P., C. Onclin, and N. Neumann (2002), Water and energy fluxes in the lower
720 Mackenzie valley, 1994/95, *Atmosphere-Ocean*, *40*(2), 245–256,
721 doi:10.3137/ao.400211.

722 McNicol, G., and W. Silver (2014), Separate effects of flooding and anaerobiosis on soil
723 greenhouse gas emissions and redox sensitive biogeochemistry, *J. Geophys. Res. ...*,
724 557–566, doi:10.1002/2013JG002433.Received.

725 Medvedeff, C. A., and A. E. Hershey (2013), Importance of methane-derived carbon as a
726 basal resource for two benthic consumers in arctic lakes, *Hydrobiologia*, *700*(1), 221–
727 230, doi:10.1007/s10750-012-1232-8.

728 Le Mer, J., and P. Roger (2001), Production, oxidation, emission and consumption of
729 methane by soils: A review, *Eur. J. Soil Biol.*, *37*(1), 25–50, doi:10.1016/S1164-
730 5563(01)01067-6.

731 Mikan, C. J., J. P. Schimel, and A. P. Doyle (2002), Temperature controls of microbial
732 respiration in arctic tundra soils above and below freezing, *Soil Biol. Biochem.*, *34*(11),
733 1785–1795, doi:10.1016/S0038-0717(02)00168-2.

734 Mitchell, C. P. J., and B. A. Branfireun (2005), Hydrogeomorphic controls on reduction-
735 oxidation conditions across boreal upland-peatland interfaces, *Ecosystems*, *8*(7), 731–
736 747, doi:10.1007/s10021-005-1792-9.

737 Mitchell, C. P. J., Branfireun, B. A., & Kolka, R. K. (2009). Methylmercury dynamics at the
738 upland-peatland interface: Topographic and hydrogeochemical controls. Water
739 Resources Research, 45(2), n/a–n/a. doi:10.1029/2008WR006832

740 Moore, T., N. Roulet, and R. Knowles (1990), Spatial and temporal variations of methane
741 flux from subarctic/northern boreal fens, *Global Biogeochem. Cycles*, *4*(1), 29–46.

742 Parkin, T. B. (1987), Soil microsites as a source of denitrification variability, *Soil Sci. Soc.*
743 *Am. J.*, *51*, 1194–1199, doi:10.2136/sssaj1987.03615995005100050019x.

744 Paytan, A., A. L. Lecher, N. Dimova, K. J. Sparrow, F. G.-T. Kodovska, J. Murray, S.
745 Tulaczyk, and J. D. Kessler (2015), Methane transport from the active layer to lakes in
746 the Arctic using Toolik Lake, Alaska, as a case study, *Proc. Natl. Acad. Sci.*,
747 201417392, doi:10.1073/pnas.1417392112.

748 Peters, V., and R. Conrad (1996), Sequential reduction processes and initiation of CH_4
749 production upon flooding of oxic upland soils, *Soil Biol. Biochem.*, *28*(3), 371–382.

750 Ponnamperuma, F. N. (1972), The Chemistry of Submerged Soils, *Adv. Agron.*, *24*(C), 29–
751 96, doi:10.1016/S0065-2113(08)60633-1.

752 Quinton, W. L., and P. Marsh (1998), The influence of mineral earth hummocks on
753 subsurface drainage in the continuous permafrost zone, *Permafr. Periglac. Process.*,
754 *9*(3), 213–228, doi:10.1002/(SICI)1099-1530(199807/09)9:3<213::AID-

PPP285>3.0.CO;2-E.

Quinton, W. L., and P. Marsh (1999), A conceptual framework for runoff generation in a permafrost environment, *Hydrol. Process.*, *13*(16 SPEC. ISS.), 2563–2581, doi:10.1002/(SICI)1099-1085(199911)13:16<2563::AID-HYP942>3.0.CO;2-D.

Quinton, W. L., and J. W. Pomeroy (2006), Transformations of runoff chemistry in the Arctic tundra, Northwest Territories, Canada, *Hydrol. Process.*, *20*(14), 2901–2919, doi:10.1002/hyp.6083.

Quinton, W. L., D. M. Gray, and P. Marsh (2000), Subsurface drainage from hummock-covered hillslopes in the arctic tundra, *J. Hydrol.*, *237*, 113–125, doi:10.1016/S0022-1694(00)00304-8.

Rabenhorst, M. C., W. D. Hively, and B. R. James (2009), Measurements of Soil Redox Potential, *Soil Sci. Soc. Am. J.*, *73*(2), 668, doi:10.2136/sssaj2007.0443.

Rampton, V. (1987), Quaternary Geology of the Tuktoyaktuk Coastlands, Northwest Territories, *Mem. 423, Geol. Surv. Canada*, 98.

Schimel, J. P. (1995), Plant transport and methane production as controls on methane flux from arctic wet meadow tundra, *Biogeochemistry*, *28*(3), 183–200, doi:10.1007/BF02186458.

Segers, R. (1998), Methane production and methane consumption: a review of processes underlying wetland methane fluxes, *Biogeochemistry*, 23–51.

Sepulveda-Jauregui, A., K. M. Walter Anthony, K. Martinez-Cruz, S. Greene, and F. Thalasso (2015), Methane and carbon dioxide emissions from 40 lakes along a north–south latitudinal transect in Alaska, *Biogeosciences*, *12*(11), 3197–3223, doi:10.5194/bg-12-3197-2015.

Seybold, C. a, W. Mersie, J. Huang, and C. McNamee (2002), Soil redox, pH, temperature,

779 and water-table patterns of a freshwater tidal wetland, *Wetlands*, *22*(1), 149–158,
780 doi:10.1672/0277-5212(2002)022[0149:SRPTAW]2.0.CO;2.

781 Skoog, D. a, D. M. West, F. J. Holler, and S. R. Crouch (1996), *Fundamentals of Analytical*
782 *Chemistry*, 7th ed., Saunders College Publishing, Fort Worth.

783 Teare (1998), Spatial and temporal patterns of chemical solute signals in sixteen small tundra
784 streams of the Trail Valley Creek watershed in the Western Canadian Arctic, Simon
785 Fraser University, Vancouver.

786 Teh, Y. A., and W. L. Silver (2006), Effects of soil structure destruction on methane
787 production and carbon partitioning between methanogenic pathways in tropical rain
788 forest soils, *J. Geophys. Res.*, *111*(G1), G01003, doi:10.1029/2005JG000020.

789 Tetzlaff, D., J. Buttle, S. K. Carey, K. McGuire, H. Laudon, and C. Soulsby (2015), Flow
790 pathways, storage and runoff generation in northern catchments: a review, *Hydrol.*
791 *Process.*, *29*(16), 3475–3490, doi:10.1002/hyp.10412.

792 Treat, C. et al. (2015), A pan-Arctic synthesis of CH_4 and CO_2 production from anoxic soil
793 incubations, *Glob. Chang. Biol.*, n/a–n/a, doi:10.1111/gcb.12875.

794 Van Bochove, E., Beauchemin S. and G. Thériault (2002), Continuous Multiple
795 Measurement
796 of Soil Redox Potential Using Platinum Microelectrodes., Soil Sci. Soc. Am. J, (66),
797 1813-1820, doi:10.2136/sssaj2002.1813.

798 Vorenhout, M., H. G. van der Geest, and E. R. Hunting (2011), An improved datalogger and
799 novel probes for continuous redox measurements in wetlands, *Int. J. Environ. Anal.*
800 *Chem.*, *91*(7-8), 801–810, doi:10.1080/03067319.2010.535123.

801 Wachinger, G., S. Fiedler, and K. Roth (2000), Variability of soil methane production on the

micro-scale: spatial, *Soil Biol. Biochem.*, *32*(8 / 9), 1121.

Waddington, J. M., and N. T. Roulet (1997), Groundwater flow and dissolved carbon movement in a boreal peatland, *J. Hydrol.*, *191*(1-4), 122–138, doi:10.1016/S0022-1694(96)03075-2.

Walter, K. M., S. A. Zimov, J. P. Chanton, D. Verbyla, and F. S. Chapin (2006), Methane bubbling from Siberian thaw lakes as a positive feedback to climate warming., *Nature*, *443*(7107), 71–5, doi:10.1038/nature05040.

Whalen, S. C., & Reeburgh, W. S. (1990). Consumption of atmospheric methane by tundra soils. *Nature*, 346(6280), 160–162. doi:10.1038/346160a0

Wik, M., B. F. Thornton, D. Bastviken, S. MacIntyre, R. K. Varner, and P. M. Crill (2014), Energy input is primary controller of methane bubbling in subarctic lakes, *Geophys. Res. Lett.*, *41*(2), 555–560, doi:10.1002/2013GL058510.Received.

Wik, M., R. K. Varner, K. W. Anthony, S. MacIntyre, and D. Bastviken (2016), Climate-sensitive northern lakes and ponds are critical components of methane release, *Nat. Geosci.*, *advance on*(2), 99–106, doi:10.1038/ngeo2578.

Wrona, F. J., M. Johansson, J. M. Culp, A. Jenkins, J. M, I. H. Myers-Smith, T. D. Prowse, W. F. Vincent, and P. A. Wookey (2016), Transitions in Arctic ecosystems: Ecological implications of a changing hydrological regime, *J. Geophys. Res. G Biogeosciences*, *121*(3), 650–674, doi:10.1002/2015JG003133.

Yu, K., F. Böhme, J. Rinklebe, H.-U. Neue, and R. D. DeLaune (2007), Major Biogeochemical Processes in Soils-A Microcosm Incubation from Reducing to Oxidizing Conditions, *Soil Sci. Soc. Am. J.*, *71*(4), 1406, doi:10.2136/sssaj2006.0155.

Zimov, S. A, Y. V Voropaev, I. P. Semiletov, S. P. Davidov, S. F. Prosiannikov, F. S. Chapin, M. C. Chapin, S. Trumbore, and S. Tyler (1997), North Siberian lakes: A

826 methane source fueled by Pleistocene carbon, *Sci. (New York, NY)*, *277*(5327), 800–802.

827

Tables

Table 1. Soil pH, depth of the organic horizon, maximum frost table depth, and extent of the saturated soil zone at each transect position.

Position	pH			O horizon depth (m)	Max frost table depth (m) ± 1σ		Mean saturated zone extent (m)	
	0.1 m	0.2 m	0.3 m		July	Aug/Sep	July	Aug/Sep
R1	5.3	-	-	0.1-0.2*	0.78 ± 0.14	0.81 ± 0.17	-	-
R2	5.1	5.2	4.8	0.1-0.2#	0.62 ± 0.03	0.59 ± 0.05	-	-
R3	5.1	4.7	-	>0.35	0.32 ± 0.01	0.35 ± 0.03	0.00	0.00
R4	5.2	5.1	-	>0.41	0.33 ± 0.04	0.41 ± 0.07	0.09	0.11
R5	5.4	5.3	5.5	0.15	0.51 ± 0.04	0.57 ± 0.08	0.11	0.17
R6	4.5	5.0	4.7	0.14	0.48 ± 0.07	0.51 ± 0.05	0.14	0.24
R7	5.4	5.3	5.3	0.20	0.50 ± 0.03	0.57 ± 0.05	0.21	0.38
R8	5.2	5.6	5.0	0.11	0.52 ± 0.08	0.48 ± 0.04	0.17	0.28
R9	4.8	5.2	5.4	0.21	0.48 ± 0.03	0.44 ± 0.03	0.13	0.19

*O horizon between 0.1-0.2 m depth. Dense root mat to depth >0.5 m
#O horizon between 0.1-0.2 m depth. Dense root mat to depth >0.3 m

Table 2. Results for best supported multiple-regression model of $\log_{10}$ (CH_4 concentration) for active layer soils and sediments. Signficance is indicated by: *** $P < 0.001$, ** $P < 0.01$, * $P < 0.05$.

Coefficients	Estimate	Std. Error
Soil depth ***	0.040	0.005
Active layer depth **	1.15	0.390
Water table depth ***	-1.73	0.345
Days Eh < +200mV ***	0.037	0.004

Residual S.E. = 0.49 (124 df); Adjusted $R^2 = 0.84$; $F_{4,124} = 163.4$; $P < 2.2e\text{-}16$.

844

845 **Figure legends**

846

847 **Figure 1.** Images of the study site **(a)** satellite image of Siksik creek catchment with redox
848 measurement transect and stream sampling locations **(b)** photograph of the redox
849 measurement transect. R1 indicates the location of the redox probe in the middle of the
850 stream channel, R9 the probe at the furthest point from the stream; the inset shows the
851 location of study site in NW Canada.

852

853 **Figure 2.** Meterological conditions during the study period: **(a)** maximum and minimum
854 daily air temperatures and average daily stream temperature, and **(b)** daily precipitation and
855 stream water discharge for Siksik Creek (where a daily discharge of 10 mm day^{-1} is
856 equivalent to an average daily discharge of 61.8 L s^{-1}).

857

858 **Figure 3** Redox potential (Eh) though time in **(a)** hillslope soils (probes R6 – R9), **(b)**
859 channel bank soils (probes R3-R5), and **(c)** in the stream water and stream channel sediments
860 (probes R1 & R2). Hatched areas indicate time periods when redox probes were disturbed so
861 no data are available. Eh at 0.1 m soil depth was > +600mV throughout thaw season at all
862 positions on the hillslope and, for clarity, these data are omitted from the figure.

863

864 **Figure 4**. Spatial patterns of redox potential (Eh) along a transect perpendicular to Siksik
865 Creek. Panels (a-d) show data from four dates through the thaw season, 24 hours prior to soil
866 profile gas sampling (see Fig 5). Redox potentials (mV) are interpolated across a regular grid
867 with respect to the ground surface using a loess smoothing function. The position and depth
868 of the probes are indicated. The middle of the stream channel is at 0 m on the x-axis. Blue
869 cross-hatching indicates the position of the saturated soil zone based on piezometer data, grey
870 represents frozen ground, white areas indicate no available data.

Figure 5. Soil methane concentrations along a transect perpendicular to Siksik Creek. Panels (a-d) show data from four dates through the thaw season. The area of each circle is proportional to the measured concentration of methane (ppm). Pink symbols show data in the range 1.8 – 250 ppm, and red symbols show data in the range 250 – 160,000 ppm. Blue cross-hatching indicates the position of the saturated soil zone based on piezometer data, and grey represents frozen ground.

Figure 6. Soil and sediment methane concentrations and relationships with environmental variables: **(a)** frequency distributions of methane concentrations for the hillslope and channel bank soils (R3-R9), **(b)** stream channel (R1 & R2) sediments, **(c)** relationship between soil/sediment methane concentrations and measurement depth, **(d)** relationship between soil/sediment methane concentrations and number of days Eh $< +200$ mV, and **(e)** measured vs. modelled methane concentrations, based on best-supported linear regression model including measurement depth, number of anaerobic days (Eh $< +200$ mV), water table depth, and thaw depth as explanatory variables.

Figure 7. (a) stream water methane concentrations through the thaw season plotted with stream water redox potential. The grey shaded area indicates the time period during which stream redox potential was $< +200$ mV, and (b) heat map of correlations between soil methane concentration and aquatic methane concentrations at each position and soil depth on the transect. Where values are given, $p < 0.05$. Correlations are only shown where $n > 4$.

Figure 8. Conceptual model of hillslope redox processes. Hatched lines indicate saturated soils/sediments. The pink shaded area indicates a transient zone of methane production which is dependent on reducing conditions developing over time during the thaw season. The red shaded area indicates a permanently reducing environment with a zone of methane produced over multiple years.

Figure 1. Figure

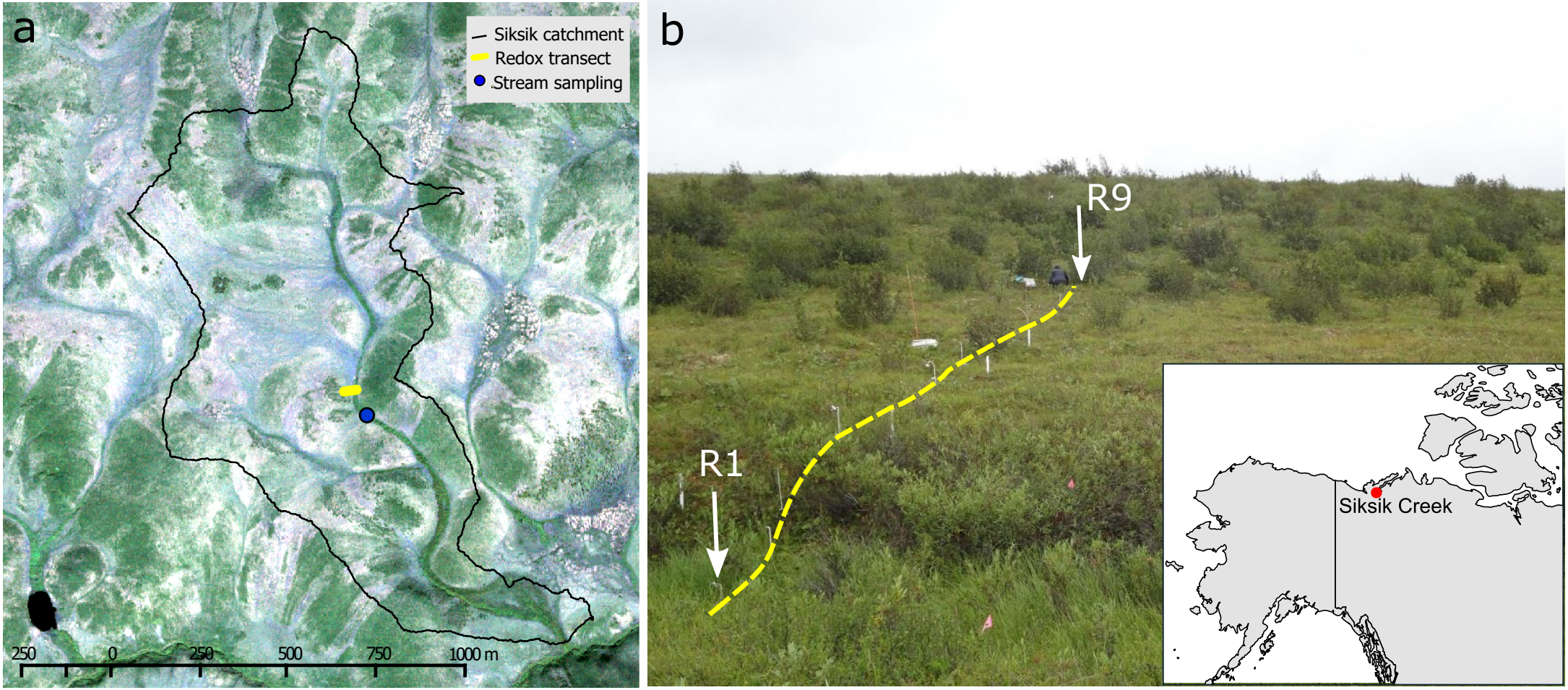
a
Siksik catchment
Redox transect
Stream sampling
250
0
250
500
750
1000 m
b
R9
R1
Siksik Creek

Figure 2. Figure

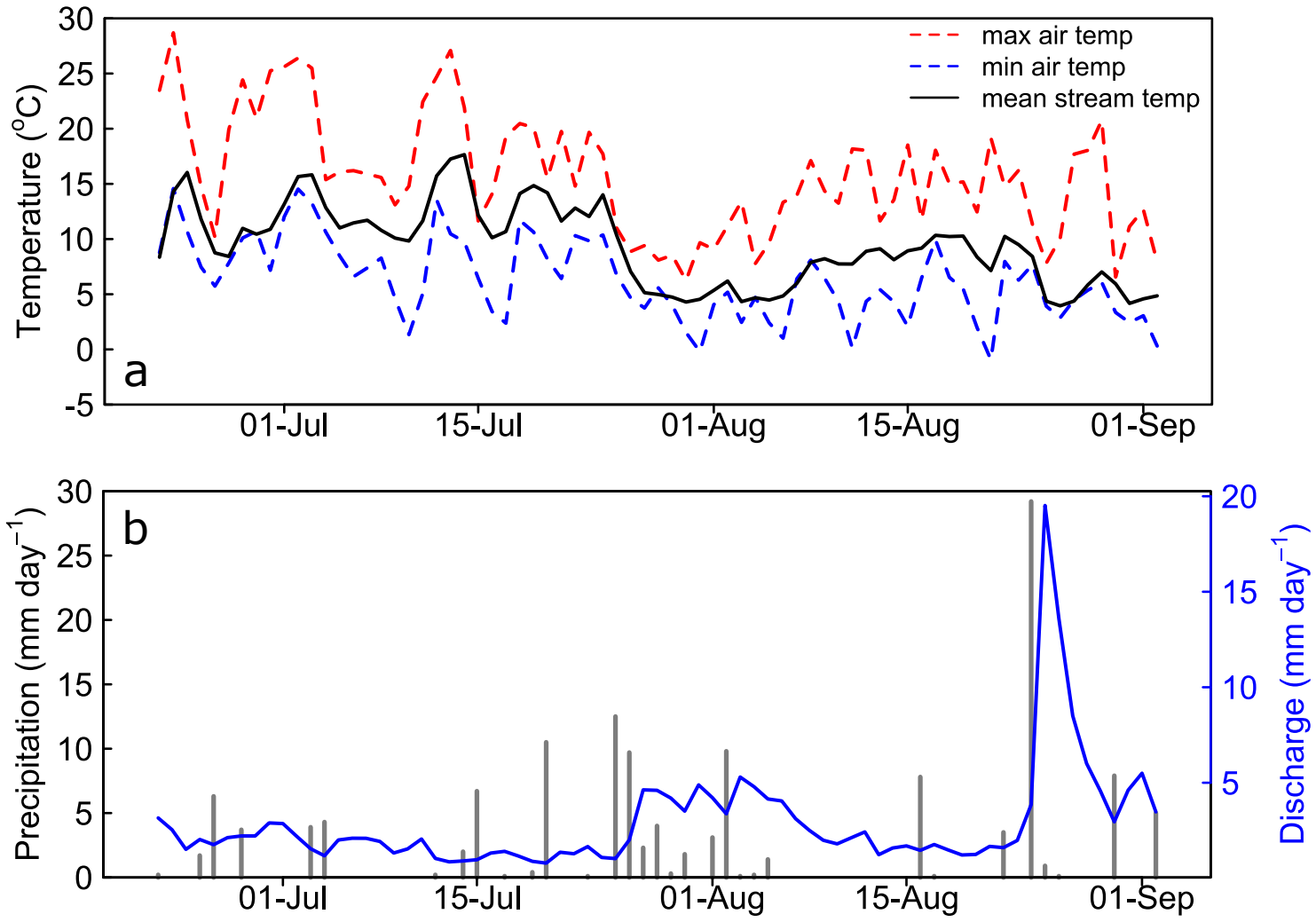
max air temp
min air temp
mean stream temp
Temperature (°C)
30
25
20
15
10
5
0
-5
a
01-Jul
15-Jul
01-Aug
15-Aug
01-Sep
b
Precipitation (mm day⁻¹)
Discharge (mm day⁻¹)
20
15
10
5

Figure 3. Figure

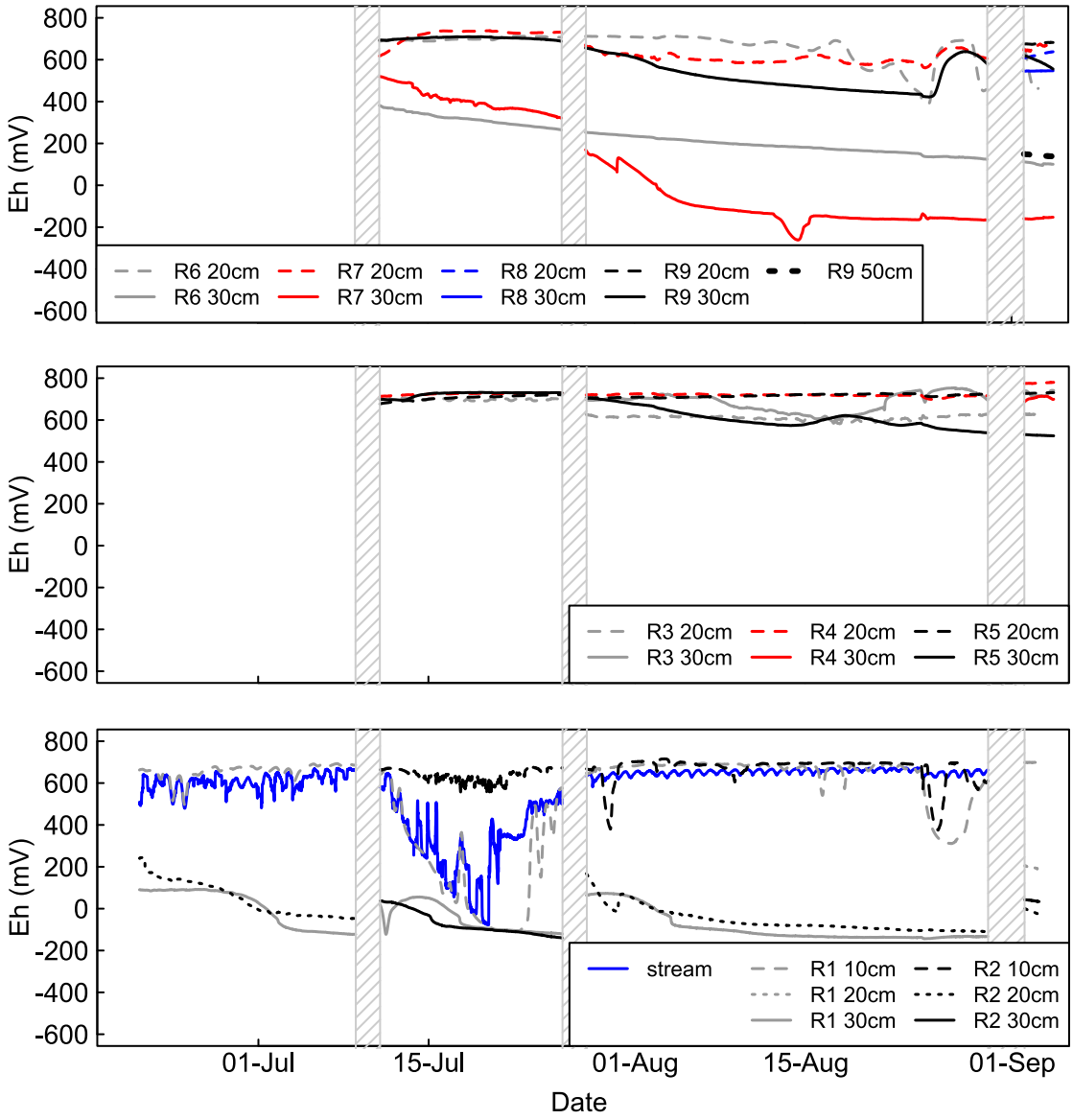
800
600
400
200
0
-200
-400
-600
Eh (mV)
R6 20cm
R6 30cm
R7 20cm
R7 30cm
R8 20cm
R8 30cm
R9 20cm
R9 30cm
R9 50cm
R3 20cm
R3 30cm
R4 20cm
R4 30cm
R5 20cm
R5 30cm
stream
R1 10cm
R1 20cm
R1 30cm
R2 10cm
R2 20cm
R2 30cm
01-Jul
15-Jul
01-Aug
15-Aug
01-Sep
Date

Figure 4. Figure

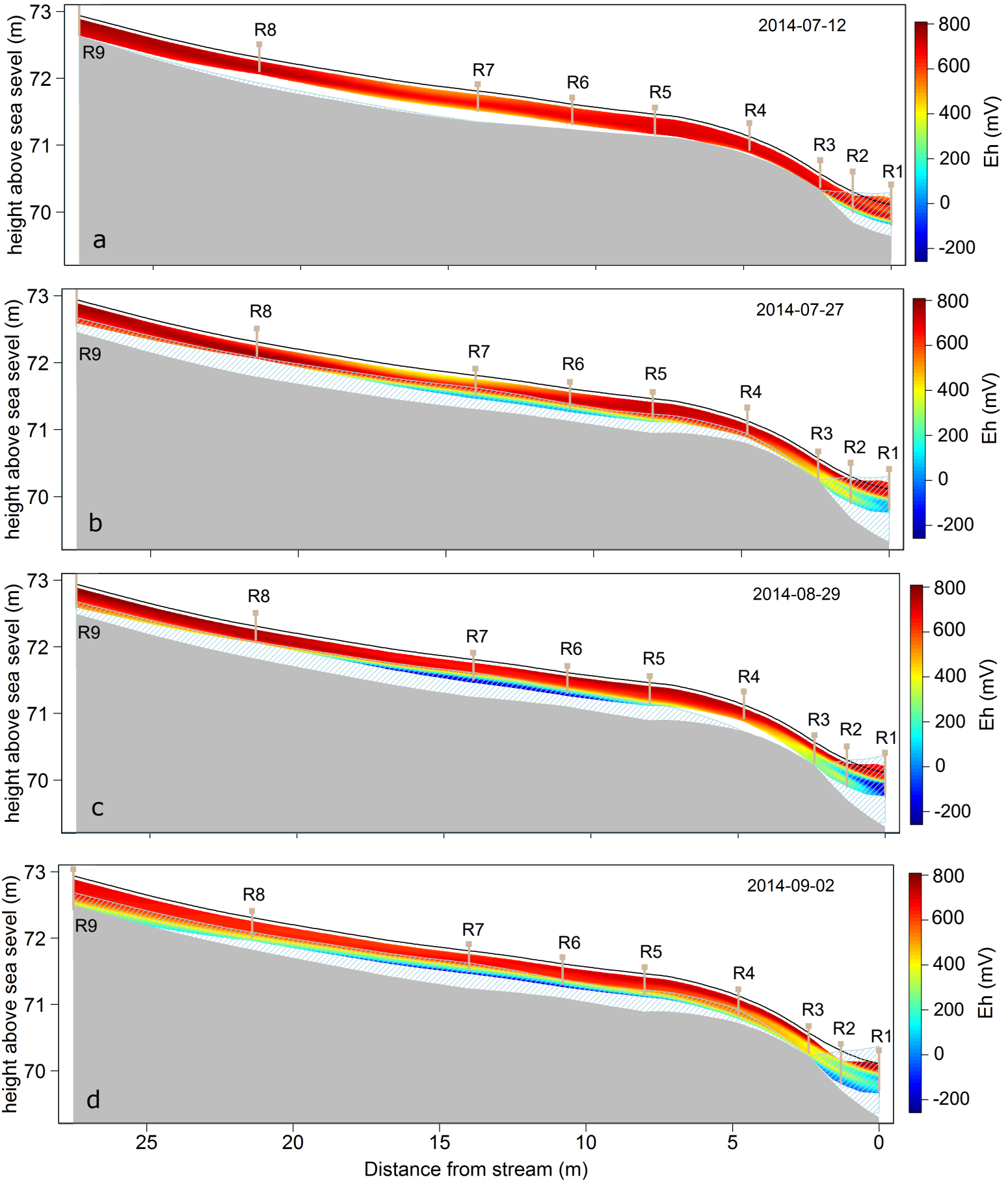
height above sea sevel (m)
73
72
71
70
R8
R9
R7
R6
R5
R4
R3
R2
R1
2014-07-12
a
2014-07-27
b
2014-08-29
c
2014-09-02
d
800
600
400
200
0
-200
Eh (mV)
25
20
15
10
5
0
Distance from stream (m)

Figure 5. Figure

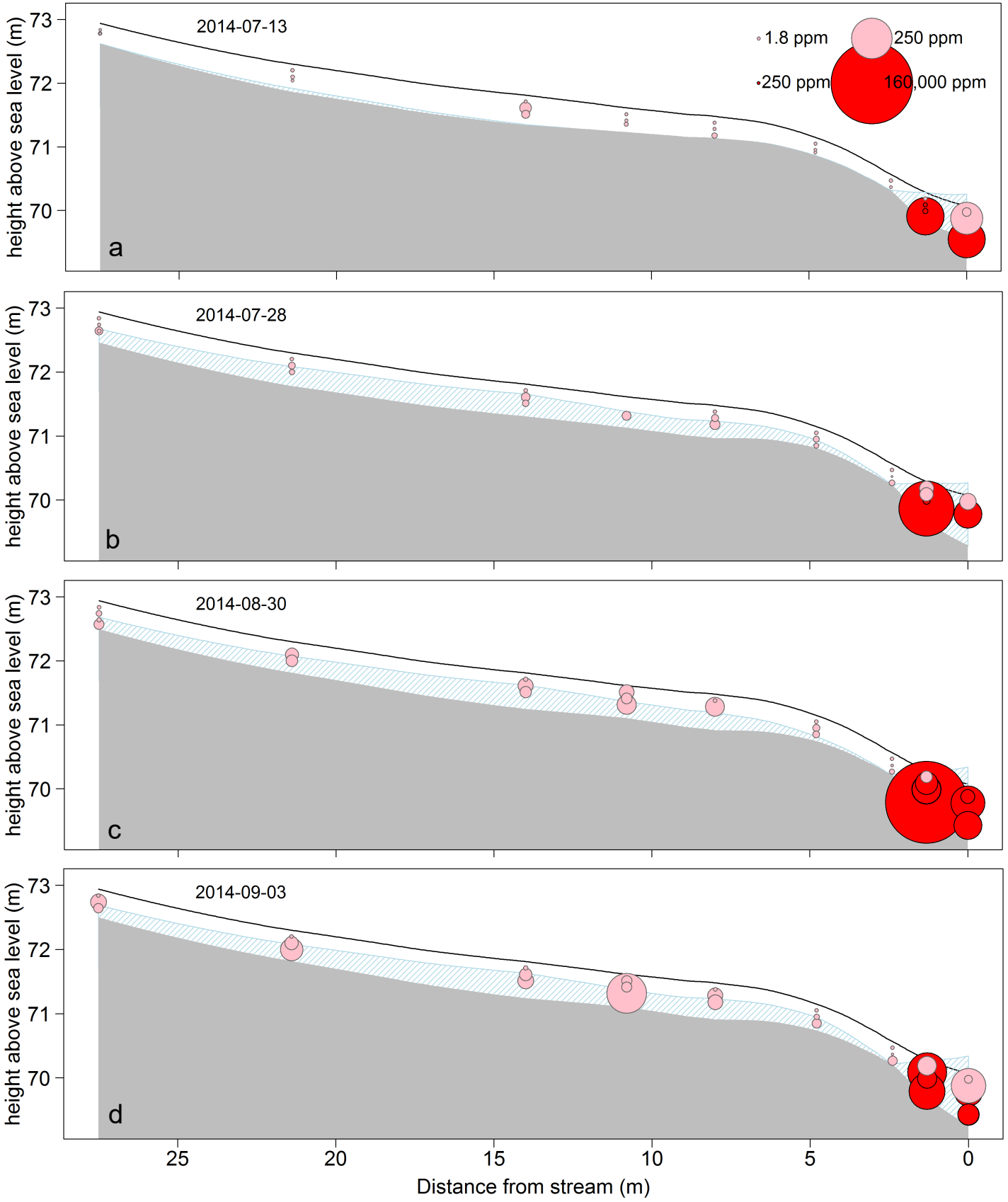
2014-07-13
1.8 ppm
250 ppm
250 ppm
160,000 ppm
a
2014-07-28
b
2014-08-30
c
2014-09-03
d
height above sea level (m)
73
72
71
70
25
20
15
10
5
0
Distance from stream (m)

Figure 6. Figure

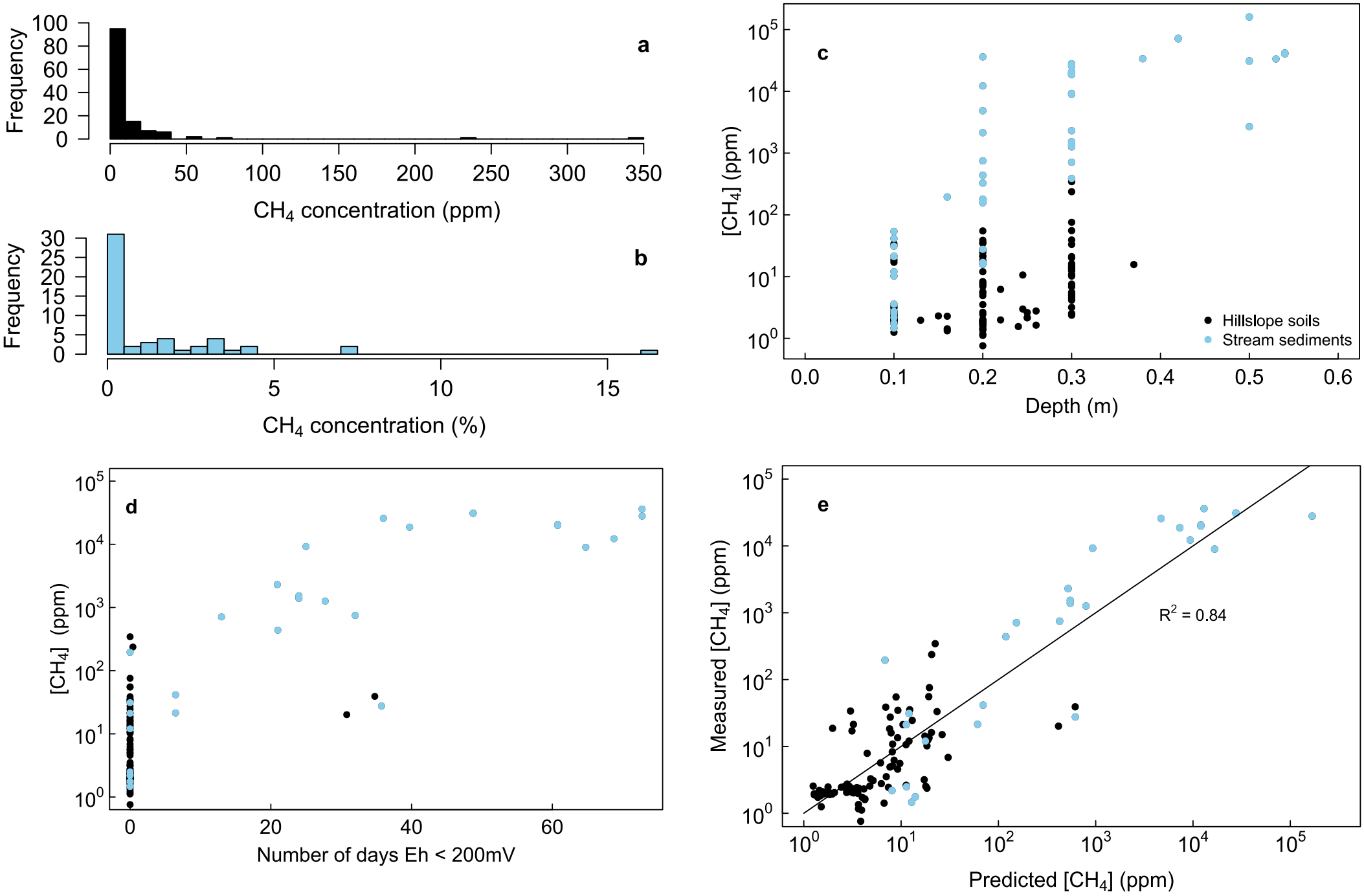
a
Frequency
100
80
60
40
20
0
0
50
100
150
200
250
300
350
CH4 concentration (ppm)
b
Frequency
30
25
20
15
10
5
0
0
5
10
15
CH4 concentration (%)
c
[CH4] (ppm)
10^5
10^4
10^3
10^2
10^1
10^0
0.0
0.1
0.2
0.3
0.4
0.5
0.6
Depth (m)
Hillslope soils
Stream sediments
d
[CH4] (ppm)
10^5
10^4
10^3
10^2
10^1
10^0
0
20
40
60
Number of days Eh < 200mV
e
Measured [CH4] (ppm)
10^5
10^4
10^3
10^2
10^1
10^0
R2 = 0.84
10^0
10^1
10^2
10^3
10^4
10^5
Predicted [CH4] (ppm)

Figure 7. Figure

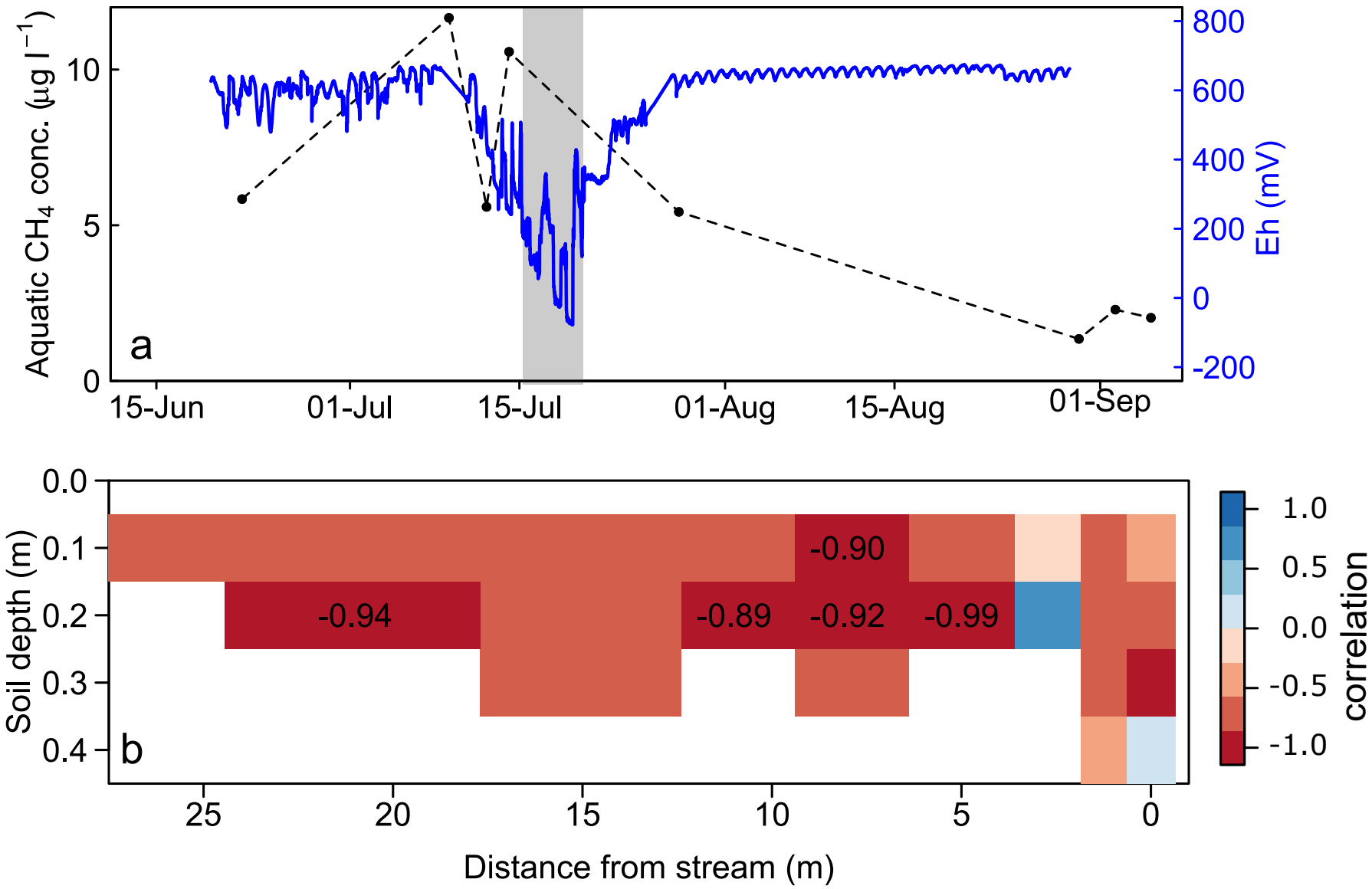
Aquatic CH_4 conc. (µg l^{-1})
10
5
0
a
15-Jun
01-Jul
15-Jul
01-Aug
15-Aug
01-Sep
800
600
400
200
0
-200
Eh (mV)
Soil depth (m)
0.0
0.1
0.2
0.3
0.4
b
-0.90
-0.94
-0.89
-0.92
-0.99
25
20
15
10
5
0
Distance from stream (m)
1.0
0.5
0.0
-0.5
-1.0
correlation

Figure 8. Figure

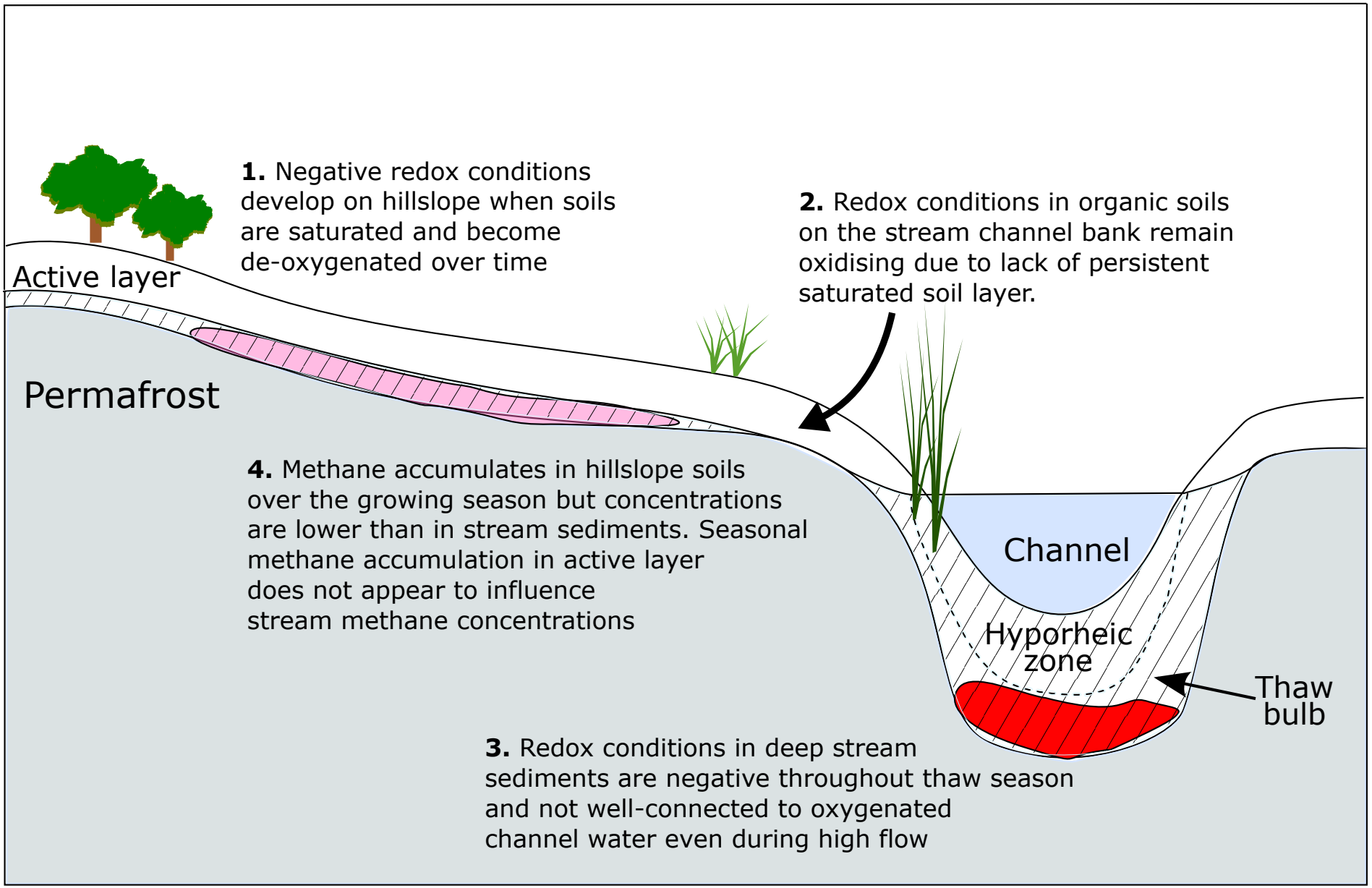
1. Negative redox conditions develop on hillslope when soils are saturated and become de-oxygenated over time
2. Redox conditions in organic soils on the stream channel bank remain oxidising due to lack of persistent saturated soil layer.
Active layer
Permafrost
4. Methane accumulates in hillslope soils over the growing season but concentrations are lower than in stream sediments. Seasonal methane accumulation in active layer does not appear to influence stream methane concentrations
Channel
Hyporheic zone
Thaw bulb
3. Redox conditions in deep stream sediments are negative throughout thaw season and not well-connected to oxygenated channel water even during high flow